frontiers | Frontiers in Food Science and Technology

TYPE Original Research
PUBLISHED 06 March 2023
DOI 10.3389/frfst.2023.1111571

OPEN ACCESS

EDITED BY
Elena Bartkiene,
Lithuanian University of Health Sciences, Lithuania

REVIEWED BY
Mohini Prabha Singh,
Punjab Agricultural University, India
Zheng-Jun Li,
Beijing University of Chemical Technology, China

*CORRESPONDENCE
Lars M. Blank,
lars.blank@rwth-aachen.de

†These authors share first authorship

SPECIALTY SECTION
This article was submitted to Food Safety and Quality Control, a section of the journal Frontiers in Food Science and Technology

RECEIVED 29 November 2022
ACCEPTED 21 February 2023
PUBLISHED 06 March 2023

CITATION
Halmschlag B, Völker F, Hanke R, Putri SP, Fukusaki E, Büchs J and Blank LM (2023), Metabolic engineering of *B. subtilis* 168 for increased precursor supply and poly-γ-glutamic acid production. *Front. Food. Sci. Technol.* 3:1111571. doi: 10.3389/frfst.2023.1111571

Metabolic engineering of *B. subtilis* 168 for increased precursor supply and poly-γ-glutamic acid production

Birthe Halmschlag[1†], Frederik Völker[1†], René Hanke[2†], Sastia P. Putri[3], Eiichiro Fukusaki[3], Jochen Büchs[2] and Lars M. Blank[1*]

[1]Institute of Applied Microbiology-IAMB, Aachen Biology and Biotechnology-ABBt, RWTH Aachen University, Aachen, Germany, [2]AVT–Aachener Verfahrenstechnik, Biochemical Engineering, RWTH Aachen University, Aachen, Germany, [3]Department of Biotechnology, Graduate School of Engineering, Osaka University, Osaka, Japan

Poly-γ-glutamic acid (γ-PGA) is an emerging biopolymer produced by several *Bacillus* species. To improve γ-PGA synthesis, metabolic engineering of the production host *B. subtilis* poses great potential and is facilitated by the convenient genetical amenability of the organism. In this study, a 3.7-fold increase in γ-PGA production using a *bdhA*, *alsSD*, *pta*, *yvmC,* and *cypX* deletion mutant with blocked by-product synthesis pathways was obtained. A detailed analysis of intracellular metabolites for reference strains and the γ-PGA-producing deletion strain identified the accumulation of pyruvate and acetyl-CoA in deletion mutants, highlighting the citrate synthase activity as an important metabolic engineering target for further metabolic flux optimization towards γ-PGA synthesis. An in-depth analysis of growth and γ-PGA production with on-line measurement techniques revealed significant variations across cultivations with deletion mutants that are likely caused by culture acidification due to pyruvate accumulation. Despite the observed acidification, the by-product deletion mutants outperformed the reference strains independent of the promoter controlling the PGA synthetase expression. The constructed deletion strains exhibit high γ-PGA production in minimal medium with glucose as sole carbon source as well as in modified Medium E reaching γ-PGA concentrations of 0.57 gL^{-1} and 14.46 gL^{-1}, respectively. The results presented in this work broaden the understanding of the microbial metabolism during γ-PGA production and will be useful to guide future metabolic engineering for improved γ-PGA production.

KEYWORDS

biopolymer, γ-PGA, *Bacillus subtilis*, metabolic engineering, metabolomics

1 Introduction

Poly-γ-glutamic acid (γ-PGA) is an industrially relevant biopolymer produced by several *Bacillus* species. γ-PGA consists of D- and/or L-glutamic acid monomers that are linked by gamma-amide bonds. As a water-soluble, non-toxic, edible, and hygroscopic polymer, γ-PGA is used in various applications including medicine (Park et al., 2021), food (Yu et al., 2018), wastewater treatment (Li et al., 2020), and agriculture (Pereira et al., 2017). γ-PGA producing strains are grouped into glutamate-dependent and glutamate-

independent producers based on their ability to produce γ-PGA only with or even without the addition of exogenous glutamate. As the glutamate for glutamate-dependent producers accounts for up to 50% of the production costs (Li et al., 2021), γ-PGA synthesis with a glutamate-independent strain is favorable for cost-effective γ-PGA production. However, to date the γ-PGA titers obtained with glutamate-independent strains are insufficient for industrial production (Sirisansaneeyakul et al., 2017).

Recently, metabolic engineering approaches aimed for increasing the γ-PGA titers with decreased production costs. To increase γ-PGA titer especially with glutamate independent strains, the main metabolic engineering targets are an increased glutamate precursor supply, the prevention of γ-PGA degradation, and the deletion of by-product synthesis routes. Approaches to enhance the precursor supply included the use of silencing RNAs to repress the expression of *rocG* encoding a glutamate dehydrogenase. The repression of *rocG* successfully increased the intracellular glutamate supply and thereby enhanced the γ-PGA production (Feng et al., 2014). Inspired by glutamate production in *Corynebacterium glutamicum*. a more energy-efficient glutamate synthesis without ATP consumption was enabled by introduction of the *C. glutamicum* glutamate synthesis machinery. Moreover, a metabolic toggle switch controlling the expression of the α-oxoglutarate dehydrogenase complex was investigated, as this operon was shown to be completely repressed during glutamate synthesis in *C. glutamicum* (Feng et al., 2017). To increase the flux from 2-oxoglutarate to glutamate, a gene deletion of *odhAB* or *sucCD*, encoding the 2-oxoglutarate dehydrogenase and the succinyl-CoA synthetase, respectively, has been studied. The deletions successfully channeled the metabolic flux towards glutamate, thereby increasing the γ-PGA titer (Massaiu et al., 2019).

Besides the increase in precursor supply, the deletion of γ-PGA depolymerases was reported to optimize the γ-PGA synthesis. Mainly, the three genes *cwlO, ggt*, and *pgdS* encoding the D, L-endopeptidase CwlO, gamma-glutamyl transferase Ggt, and the gamma-D, L-glutamyl hydrolase PgdS, respectively, were studied in various *Bacillus* strains, highlighting strain-specific differences in the effect of the gene deletions. While the double deletion of *pgdS* and *ggt* improved the γ-PGA synthesis in a *B. subtilis* strain (Scoffone et al., 2013), the same deletions had no effect in *B. amyloliquefaciens*. However, the double deletion of *pgdS* and *cwlO* increased the production in *B. amyloliquefaciens* (Feng et al., 2014). The detailed analysis of single, double, and the triple deletion mutant of the genes *cwlO, ggt*, and *pgdS* in *B. subtilis* using on-line measurement of oxygen transfer rate (OTR) and viscosity recently identified the triple gene deletion as a beneficial modification for γ-PGA synthesis in glucose minimal medium (Hoffmann et al., 2022).

The main by-products during γ-PGA synthesis with *B. subtilis* in a medium containing glucose, yeast extract, and glutamic acid are 2,3-butanediol and acetoin. Furthermore, minor amounts of acetate and lactate are formed (Zhu et al., 2013). To prevent by-product synthesis and thereby increase γ-PGA production, the deletion of the genes involved in 2,3-butanediol and acetoin production, *bdhA* and *alsSD*, respectively, are major engineering targets. The deletion of *pta*, encoding the phosphotransacetylase that is involved in the synthesis of the by-product acetate, was reported to slightly increase γ-PGA production in *B. amyloliquefaciens* (Feng et al., 2015). Feng et al. (2015) further reported a beneficial effect for the deletion of the *eps* and *lps* operons that are responsible for the synthesis of extracellular polysaccharides and lipopolysaccharides, respectively.

In recent years, rational approaches enabled great progress in the design of whole-cell biocatalysts (Lin and Tao, 2017). These rational approaches were greatly accelerated through the integration of omics data (Amer and Baidoo, 2021). Among these omics technologies, the field of metabolomics is particularly useful to guide metabolic engineering approaches (Putri et al., 2013). Metabolomics studies were successfully applied over a wide range of organisms and products, covering, e.g., amino acid production in yeast (Gold et al., 2015), flavonoid production in tomatoes (Bovy et al., 2007), and biofuel production in microalgae and cyanobacteria (Kato et al., 2022). These examples highlight metabolome analysis as an important tool to guide rational approaches towards metabolic bottlenecks and promising engineering targets. This can also be applied to improve the γ-PGA synthesis with *B. subtilis*.

This study focused on further improving γ-PGA synthesis of a glutamate-independent *B. subtilis* 168 derivative (Halmschlag et al., 2019) using glucose as sole carbon source. Minimizing by-product formation was here chosen as Metabolic Engineering target, resulting in strain *B. subtilis* ΔBP (delta by-products) with deletions of genes *bdhA*, *alsSD*, *pta*, *yvmC,* and *cypX*. An in-depth analysis of *B. subtilis* ΔBP variant PG3 using on-line viscosity measurements and metabolome analysis was carried out to identify strain characteristics and potentially further metabolic engineering targets. Efficient γ-PGA synthesis was demonstrated using modified Medium E that is frequently used for γ-PGA production. The study highlights the value of combining metabolic engineering and in-depth strain characterization for resource- and cost efficient γ-PGA production.

2 Materials and methods

Reagents. D-Glucose, L-glutamic acid, NH_4Cl, K_2HPO_4, $MgSO_4{\cdot}7H_2O$, $CaCl_2{\cdot}2H_2O$, $MnSO_4{\cdot}H_2O$, $FeCl_3{\cdot}6H_2O$, $ZnSO_4{\cdot}7H_2O$, Na_2-EDTA, $CuSO_4{\cdot}5H_2O$ and $CoCl_2{\cdot}6H_2O$ were purchased from Carl Roth GmbH + Co. KG (Karlsruhe, Germany). LC/MS-grade ultra-pure water, HPLC-grade chloroform, acetic acid, H_2SO_4 and NH_4HCO_3 were purchased from Wako Pure Chemical Industries, Ltd. (Osaka, Japan). 10-Camphorsulfonic acid and tributylamine were purchased from SigmaAldrich (MO, United States).

Strains, plasmids and growth conditions. The bacterial strains and plasmids used and constructed in this study are listed in Table 1. All cloning steps were carried out in *E. coli* DH5α. The recombinase positive *E. coli* strain JM101 was used for plasmid propagation prior to the transformation of *B. subtilis*. The previously reported strain *B. subtilis* Δspo (Halmschlag et al., 2019) that is a derivative of the *manP*A-negative strain *B. subtilis* IIG-Bs2 (Wenzel and Altenbuchner, 2015) was used as starting strain for metabolic engineering.

For plasmid construction and counter selection, strains were cultivated at 37°C in LB medium containing 100 μg/mL spectinomycin or 0.5% (w/v) mannose when required. For γ-PGA production and metabolome analysis, the *B. subtilis* strains were grown in glucose minimal medium. The bacterial strains and plasmids used and created in this study are listed in Table 1.

Deletion plasmid construction. The plasmids used for the deletion of genes and integration of the promoter upstream of

TABLE 1 Strains and plasmids used in this study.

Strain	Genotype/properties	References/source
Strains		
E. coli DH5α	*fhuA*2 Δ(*argF-lacZ*)U169 *phoA glnV*44 Φ80 Δ(*lacZ*)M15 *gyrA*96 *recA*1 *relA*1 *endA*1 thi-1 hsdR17	Meselson and Yuan (1968)
E. coli JM101	*glnV*44 thi-1 Δ(*lac-proAB*) F'[$lacI^qZ\Delta M15$ *traD*36 $proAB^+$]	Messing et al. (1981)
B. subtilis IIG-Bs2	ΔSPβ Δ*skin* ΔPBSX ΔproΦ1 Δ*pks*::CmR, ΔproΦ3 *trp*+ Δ*manPA*::*erm* Δ*bpr* Δ*sigG* Δ*sigE* Δ*spoGA*	Wenzel and Altenbuchner (2015)
B. subtilis Δspo	Δ*bpr* Δ*sigG* Δ*sigE* Δ*spoGA*	Halmschlag et al. (2019)
B. subtilis ΔBP	as Δspo plus Δ*bdhA* Δ*alsSD* Δ*pta* Δ*yvmC* Δ*cypX*	This study
B. subtilis PG2	as Δspo plus P_{pst}-*pgs*	This study
B. subtilis PG3	as Δspo plus P_{pst}-*pgs* Δ*bdhA* Δ*alsSD* Δ*pta* Δ*yvmC* Δ*cypX*	This study
B. subtilis PG32	as Δspo plus $P_{PV35.26}$-*pgs*	This study
B. subtilis PG33	as Δspo plus $P_{PV35.26}$-*pgs* Δ*bdhA* Δ*alsSD* Δ*pta* Δ*yvmC* Δ*cypX*	This study
B. subtilis PG4	as Δspo plus Δ*xylAB*	This study
B. subtilis PG44	as PG4 plus P_{xyl}-*pgs*	Strain *B. subtilis* PG10 as described in Halmschlag et al. (2019)
B. subtilis PG5	as ΔBP plus Δ*xylAB* Δ*ldh*	This study
B. subtilis PG55	as PG5 plus P_{xyl}-*pgs*	This study
Plasmids		
pJOE-8739	Backbone for markerless counterselection system	Wenzel and Altenbuchner (2015)
pBs-9	Deletion of *alsSD*; integrative vector for *B. subtilis*, SpcR, *manP*	This study
pBs-10	Deletion of *bdhA*; integrative vector for *B. subtilis*, SpcR, *manP*	This study
pBs-11	Deletion of *pta*; integrative vector for *B. subtilis*, SpcR, *manP*	This study
pBs-14	Deletion of *cypX* and *yvmC*; integrative vector for *B. subtilis*, SpcR, *manP*	This study
pBs-17	Deletion of *xylAB*; integrative vector for *B. subtilis*, SpcR, *manP*	Halmschlag et al. (2020a)
pBS-4	P_{pst} promoter integration upstream of *pgs*; integrative vector, SpcR, *manP*	Hoffmann et al. (2022)
pBS-2	P_{xyl} promoter integration upstream of *pgs*; integrative vector, SpcR, *manP*	Halmschlag et al. (2020b)
pBs-46	Deletion of *ldh*; integrative vector for *B. subtilis*, SpcR, *manP*	This study

the *pgs* operon were assembled using the NEB HiFi DNA Assembly Kit (NEB, Frankfurt am Main, Germany). For the integration of the P_{pst} or P_{xyl} promoter, the promoter sequences were amplified from *B. subtilis* 168 genomic DNA with the primer pairs BS-019/BS-020 or BS-009/BS-010 (see Supplementary Table S1). The two target sequences (TS) for integration and subsequent removal of the plasmid were amplified from *B. subtilis* 168 genomic DNA, using the primer pairs BS-068/BS-069 and BS-070/BS-071 for P_{pst} integration or TS1_fwd/TS1_rev and TS2_fwd/TS2_rev for P_{xyl} integration. The TS1 and TS2 regions for the deletion of the genes *alsSD*, *bdhA*, *pta*, *yvmC* and *cypX*, *xylAB,* and *ldh* were amplified similarly by using the primer pairs BS-029/BS-030 and BS-031/BS-032, BS-033/BS-034 and BS-035/BS-036, BS-037/BS-038 and BS-039/BS-040, BS-053/BS-054 and BS-055/BS-056, BS-085/BS-086 and BS-087/BS-088 as well as BS-325/BS-326 and BS-327 and BS-328, respectively. The fragments were assembled with the vector backbone pJOE-8739 linearized by BS-020/BS-021. Vector assembly with NEB HiFi DNA assembly was performed as described by the manufacturer. The assembled plasmids were transformed into chemically competent *E. coli* DH5α cells. Correctly constructed plasmids as confirmed by PCR were sequenced and retransformed to *E. coli* JM101 to obtain the plasmids for *B. subtilis* transformation.

Strain development. The strain *B. subtilis* Δspo was transformed with the constructed deletion plasmids to delete the genes and integrate the promoter. The transformation was performed according to the Paris Method (Harwood and Cutting, 1990). Deletions were carried out by the markerless gene deletion system from Wenzel and Altenbuchner (Wenzel and Altenbuchner, 2015). Briefly, transformed cells were selected on LB agar plates containing spectinomycin. Afterwards, the counterselection with mannose containing agar plates was used to select for cells that lost the plasmid by homologous recombination during incubation in LB without selection pressure. The plasmid loss was confirmed by both spectinomycin sensitivity of the cells and by colony PCR, while the successful deletion of genes or integration of the promoter upstream of *pgs* was confirmed by sequencing.

Cultivation for metabolite analysis. The main cultures of *B. subtilis* for the analysis of growth and metabolites were carried out in a glucose minimal medium as previously described (Halmschlag et al., 2020b). The minimal medium contained per liter: 20 g glucose, 41.9 g MOPS buffer, 7 g NH_4Cl, 0.5 g KH_2PO_4, 0.5 g $MgSO_4$, 0.15 g $CaCl_2$, 0.1 g $MnSO_4$, 0.04 g $FeCl_3$ and 1 mL of a trace element solution. The trace element solution (modified trace element solution after Wenzel et al. (Wenzel et al., 2011)) contained per liter: 0.54 g $ZnSO_4 \times 7$ H_2O, 30.15 g Na_2-EDTA, 0.48 g $CuSO_4 \cdot 5$ H_2O and 0.54 g $CoCl_2 \cdot 6$ H_2O. The pH of the medium was set to 6.8 with NaOH. The two step precultures were cultivated first on LB medium overnight and second in medium identical to the main culture medium. The LB medium contained per liter: 10 g tryptone, 5 g yeast extract and 10 g NaCl at pH 7.4. The main cultures were inoculated to an OD_{600} of 0.1 from the preculture. The cultures were incubated on a rotary shaker at 37°C with shaking at 200 rpm (25 mm shaking diameter) for experiments in glucose minimal medium (Infors Multitron, Bottmingen, Switzerland). If not stated differently, all cultivations were performed in triplicate, and the reported data represent the mean values.

Cultivation in Medium E. Moreover, γ-PGA production in modified Medium E was investigated, which was modified according to Leonard et al. (Leonard et al., 1958) and ultimately composed of per liter: 30 g glycerol, 15 g citrate, 20 g L-glutamate, 4 g NH_4Cl, 0.5 g K_2HPO_4, 0.5 g $MgSO_4{\cdot}7H_2O$, 0.04 g $FeCl_3{\cdot}6H_2O$, 0.15 g $CaCl_2{\cdot}2H_2O$, 0.104 g $MnSO_4{\cdot}H_2O$, 41.9 g MOPS buffer (Mitsunaga et al., 2016). 30 g L^{-1} xylose was added to experiments with *B. subtilis* PG44 and PG55 at the beginning of the cultivation to induce expression of *pgs* based on the xylose-inducible promoter P_{xyl} (Halmschlag et al., 2020b). The pH of Medium E was adjusted to 7.2 using 10 M NaOH. Precultures were performed as indicated above. The cultures were incubated on a rotary shaker at 37°C with shaking at 300 rpm (50 mm shaking diameter) for experiments in Medium E (Infors Multitron, Bottmingen, Switzerland). All cultivations were performed in triplicate, and the reported data represent the mean values.

Biomass monitoring. The biomass concentration was determined by OD_{600} measurements of samples taken from the shake flasks using a cell density meter (Amersham Bioscience, Little Chalfont, UK). Additionally, cell growth was monitored online with a Cell Growth Quantifier (CGQ; Scientific Bioprocessing (SBI), Baesweiler, Germany). The biomass concentration is given as cell dry weight (CDW) calculated from the OD_{600} using the following correlation equation that was determined empirically: CDW [g L^{-1}] = 0.5381*OD_{600} + 0.0074. The correlation of optical density and cell dry weight was determined for the reference strain *B. subtilis* Δspo. Various dilutions of fermentation broth were prepared in triplicates and the OD_{600} was determined for each dilution. A certain volume of cell suspension that was adjusted to the biomass concentration, was centrifuged to obtain a cell pellet. The pellet was resuspended in 100 µL of 0.9% NaCl solution. The concentrated cell suspension was applied to a cellulose filter of known weight that was dried at 60°C for more than 24 h. The biomass dry weight was determined after drying the filter for 24 h to determine the correlation of CDW and OD_{600}.

Cultivation for on-line monitoring (OTR and viscosity measurements). On-line monitoring of the respiration activity determining the oxygen transfer rate (OTR) with the Respiration Activity Monitoring System (RAMOS (Anderlei and Büchs, 2001; Anderlei et al., 2004)) was carried out for the main cultures as previously described (Halmschlag et al., 2020a). Commercial versions of this system are available from Kuhner AG, Birsfelden, Switzerland or HiTech Zang, Herzogenrath, Germany.

The first pre-culture in LB medium was inoculated from 200 µL of cryo stocks. After 5 h cultures were harvested, centrifuged at 11,000 rpm, 4°C for 5°min, resuspended in minimal medium, set to an OD_{600} of 0.1 and used for the second pre-culture. The second pre-culture was harvested after 24 h of cultivation, centrifuged at 11,000 rpm, 4°C for 5°min, resuspended in minimal medium, set to an OD_{600} of 0.1 and used to start the main culture. The main culture was transferred to RAMOS flasks for on-line measurement and to additional Erlenmeyer flasks for off-line samples. The culture conditions for pre-cultures and the main culture were as follows: 250 mL shake flasks, filling volume 20 mL, shaking frequency 350 rpm, shaking diameter 50 mm, temperature 37°C, initial OD_{600} = 0.1.

The on-line viscosity measurement was carried out using a device developed by Sieben et al. (2019) as previously described (Halmschlag et al., 2020a; Hoffmann et al., 2022).

Batch fermentation. Batch fermentations were carried out in stirred tank bioreactors (BioFlo120; Eppendorf, Hamburg, Germany) as previously described (Halmschlag et al., 2019). Cell growth was monitored on-line using the cell growth quantifier for bioreactors (CGQ BioR; Scientific Bioprocessing (SBI)), where indicated and wherever, the culture conditions were kept constant with the shake flask experiments: a temperature of 37°C and an initial OD_{600} of 0.1. The pH was controlled at pH seven by the addition of 2 M HCl or 2 M NaOH. The filling volume was 0.5 L, the aeration rate was set to one vvm, and the stirrer speed was at 800 rpm.

Analysis of γ-PGA with CTAB. The γ-PGA production was analyzed using the cetyltrimethylammonium bromide (CTAB) assay as previously described (Halmschlag et al., 2019). Briefly, cells were separated by centrifugation (20 min, 5,000 g, 4°C). Subsequently, three-times the sample volume of pure ethanol was used to precipitate the γ-PGA. The precipitated γ-PGA was resuspended in distilled water. For measurement, the γ-PGA sample was mixed with CTAB solution, and the turbidity was measured at 400 nm with a Synergy MX microplate reader (BioTek Instruments, Winooski, United States). The γ-PGA concentration was calculated based on a calibration curve using standards of 1 MDa γ-PGA (Henkel AG and Co. KGaA, Düsseldorf) in the range of 0.1–10 µg mL^{-1}.

Analysis of γ-PGA with GPC. The concentration and molecular weight of γ-PGA was determined by gel permeation chromatography (GPC) as previously described (Halmschlag et al., 2020b). The GPC system (HLC-8320GPC) was equipped with a TSKgel GMPWxl column (300 × 7.8°mm, Tosoh Bioscience GmbH, Stuttgart, Germany) and a TSKgel PWxl guard column (40 × 6 mm, Tosoh Bioscience). The mobile phase used was 30 mM KNO_3 at a flow rate of 1 mL min^{-1}. The temperature of the GPC system was maintained at 40°C, and 30 µL of each purified, filtered γ-PGA sample was injected. To determine the concentration of γ-PGA in the samples, γ-PGA sodium salt was used as standard. The calibration curve for the molecular weight determination was established using poly(styrene sulfonate) sodium salt standards with a peak molecular weight (Mp) in the range of 4.21–976 kDa (PSS Polymer Standards Service GmbH, Mainz, Germany).

Analysis of glucose, acetoin, 2,3-butanediol and acetate. The consumption of glucose and production of by-products such as acetoin, 2,3-butanediol and acetate was analysed by HPLC-RI using the GL-7400 device coupled with a column oven GL-7432 (GL Science, Tokyo, Japan). The HPLC system was equipped with an Aminex HPX-87H column (7.8 × 300 mm, Bio-Rad, CA, United States). 5 mM H_2SO_4 was used as a mobile phase at a flow rate of 0.6 mL min^{-1} for 25 min. The column oven temperature was kept at 65°C. Cell-free culture supernatant was filtrated with a Mini-Uni prep PTFE filter (pore size 0.45 mm, GE Healthcare UK). 10 µL of the filtrate were injected to the HPLC system. The concentration of extracellular pyruvate was quantified using the Amplite® Colorimetric Pyruvate Assay Kit (Cat# 13821, AAT Bioquest, California, United States) according to the manufacturer's instructions. The concentration of analytes was calculated by calibrations curves established for all standards.

Sample Preparation for metabolome analysis. For metabolome analysis, culture samples were harvested during the exponential phase. The samples were prepared as previously described

(Halmschlag et al., 2020a). Briefly, a constant biomass concentration was filtered with a PVDF filter (pore size, 0.45 mm) using a vacuum. After washing the sample with 300 mM NH_4HCO_3, the cellular metabolism was quenched by soaking the filter in liquid N_2. The samples were stored at −80°C until metabolite extraction. The metabolites were extracted with 1.875 mL of extraction solvent (1:2:2, H_2O:MeOH:chloroform, including 7 nM 10-camphorsulfonic acid as internal standard) per sample. The extracted metabolites were obtained by centrifugation and supernatant was transferred to a clean tube, vacuum concentrated, and freeze-dried overnight. The obtained pellet was stored at −80°C until analyzed by LC-MS.

Ion-pair-LC/MS/MS Analysis. The extracted metabolite samples were analyzed by ion-pair-liquid chromatography coupled with tandem mass spectrometry (LC/MS/MS) analysis was performed using a Shimadzu Nexera UHPLC system coupled with an LCMS 8030 Plus device (Shimadzu Co., Kyoto, Japan). As previously described (Halmschlag et al., 2020a), the system was equipped with a PE-capped CERI L-column 2ODS column (2.1 mm × 150 mm, particle size 3 mm; Chemicals Evaluation and Research Institute, Tokyo, Japan). For the mobile phase, a gradient of a mixture of solvent A and B was used, where solvent A was 10 mM tributylamine and 15 mM acetate in ultra-pure water and solvent B was pure methanol. The flow rate was set to 0.2 mLmin^{-1}. For gradient elution of metabolites, the concentration of B was increased from 0 to 15% after 1 min with a gradient of 30% min^{-1}, held for 1.5 min, increased to 50% over 5 min and subsequently increased to 100% within 2 min. The 100% solvent B concentration was held for 1.5 min, decreased to 0% from 11.5 min on and then held at this concentration for 8.5 min. The column oven temperature was set to 45°C. The MS parameters were as follows: probe position, þ1.5°mm; desolvation line temperature, 250°C; drying gas flow, 15 L min^{-1}; heat block temperature, 400°C; and nebulized gas flow, 2 L min^{-1}. Per sample, 3 µL was injected into the ion-pair-LC/MS/MS for metabolite analysis. The samples for analysis were obtained by resuspending dried metabolite extraction samples in 50 µL of ultra-pure water.

Metabolite data processing and analysis. For metabolite data analysis, the peak area was calculated using MRMPROBS ver. 2.38 and was checked manually. The data were normalized according to the peak area of the internal standard, 10-camphorsulfonic acid. SIMCA 13 (Umetrics, Umeå, Sweden) was used for principal component analysis (PCA) and orthogonal partial least square discriminant analysis (OPLS-DA). The t-tests were performed using MATLAB (MathWorks, MA, United States).

3 Results

To improve γ-PGA synthesis in *B. subtilis* with glucose as sole carbon source, the carbon flux must be directed towards the TCA cycle and ultimately glutamate to ensure sufficient precursor supply for the γ-PGA synthetase. The resulting strain with impaired by-product synthesis was analysed in detail using a metabolomics approach and online viscosity measurements. Increased γ-PGA production with either glucose as sole carbon source or with the γ-PGA production Medium E and additional metabolic engineering targets are presented.

3.1 Prevention of by-product formation

B. subtilis produces 2,3-butanediol, acetoin, and acetate during growth on glucose. Under conditions with high γ-PGA production, lactate formation has been additionally observed. During cultivations in iron-containing minimal media also, the synthesis of pulcherriminic acid was reported (Uffen Robert and Canale-Parola, 1972). To minimize by-product formation and reroute flux towards glutamate, the formation of 2,3-butanediol, acetoin, acetate, and pulcherriminic acid was prevented by deleting the respective genes *bdhA, alsSD, pta, yvmC,* and *cypX* (Figure 1).

The influence of *bdhA, alsSD, pta, yvmC,* and *cypX* deletions on γ-PGA production was investigated by comparing two strains, *B. subtilis* PG2 (γ-PGA-producing reference without gene deletions) and *B. subtilis* PG3 (γ-PGA-producing deletion mutant) according to their growth behaviour and γ-PGA production in batch fermentations with glucose as carbon source (Figure 2). The phosphate-starvation inducible promoter was used for expression of the PGA synthetase genes *pgs*. The use of promoter P_{pst} enables the decoupling of growth and γ-PGA production and thereby allows the regulation of γ-PGA production by controlling the phosphate availability in the medium. Due to the use of the phosphate-starvation inducible promoter P_{pst}, fermentations were carried out with reduced phosphate concentrations of 0.5 g L^{-1} K_2HPO_4. Under phosphate-limited conditions, the growth appeared to be slower than in standard medium. Moreover, non-exponential growth was observed. A maximum biomass concentration of 7.1 g L^{-1} and 2.8 g L^{-1} for *B. subtilis* PG2 and *B. subtilis* PG3, respectively, was reached. A sharp drop of biomass concentration was observed for *B. subtilis* PG2 for which the CDW decreased from 7.1 g L^{-1} after 14 h to 2.5 g L^{-1} after 28 h, while the biomass concentration for *B. subtilis* PG3 was more stable throughout the stationary phase. For *B. subtilis* PG2, the γ-PGA concentration was below the detection limit up to 15 h of cultivation time. From 15 h on, only minor γ-PGA concentrations below 0.1 g L^{-1} were detectable by GPC. γ-PGA production with the deletion mutant *B. subtilis* PG3 was significantly higher, reaching a maximal titer of 0.26 g L^{-1} at the end of the cultivation corresponding to 0.089 $g_{\gamma\text{-PGA}}$ g_{CDW}^{-1} and 0.028 $g_{\gamma\text{-PGA}}$ g_{CDW}^{-1} for deletion mutant *B. subtilis* PG3 and reference PG2, respectively. The deletion of five genes to prevent by-product synthesis resulted in a 3.7-fold increase of γ-PGA production, indeed allowing the rerouting of glucose catabolism to product formation. Comparably, the absolute γ-PGA titers under the given cultivation conditions are low.

To further investigate the growth kinetics and γ-PGA production of the constructed strains *B. subtilis* PG2 and *B. subtilis* PG3, an in-depth investigation with on-line oxygen transfer rate (OTR) measurement to follow the bacterial growth, online viscosity measurement to quantify γ-PGA production, and offline sampling for biomass determination and HPLC measurements of by-product synthesis was carried out. The analysis was performed in shake flasks with the same medium with low potassium phosphate concentration that was used for the batch cultivations in bioreactors. The production was carried out as four independent cultivations each with two cultures per strain. In each of four cultivations, two shake flasks per strain were inoculated from the same preculture. However, for the deletion

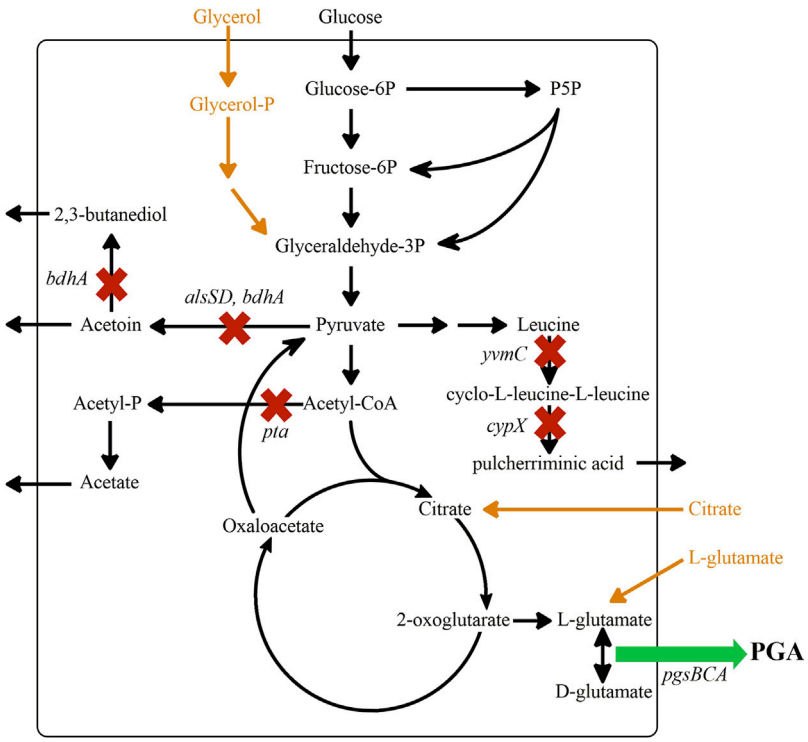

FIGURE 1
Metabolic engineering targets improving the flux towards γ-PGA. The schematic overview shows the main metabolic pathways for γ-PGA synthesis from glucose. Pathways for additional substrates as in medium E are indicated in orange. The genes *alsSD, bdhA, pta, yvmC* and *cypX* were deleted to prevent by-product formation. The PGA synthetase produces γ-PGA from L- and D-glutamate. The membrane bound synthetase complex encoded by *pgsBCA* was expressed under control of either the phosphate-starvation promoter P_{pst} or the strong xylose-inducible promoter P_{xyl}.

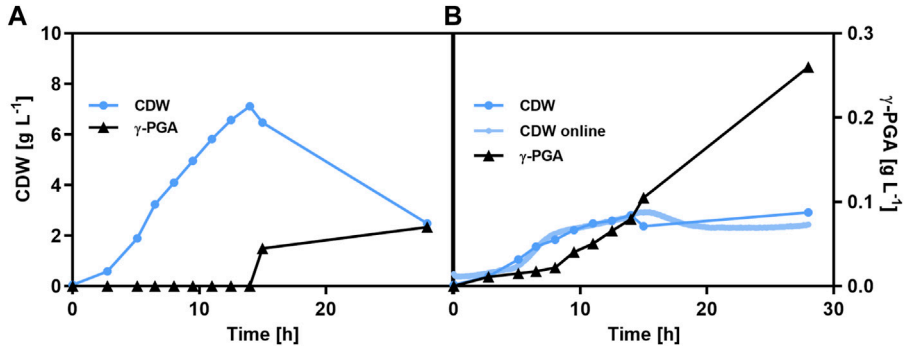

FIGURE 2
γ-PGA production of *B. subtilis* PG2 **(A)** and *B. subtilis* PG3 **(B)** under phosphate-limiting conditions. Batch cultivation of *B. subtilis* PG2 (parental strain, P_{pst}-*pgs*) and *B. subtilis* PG3 (by-product pathway deficient strain, P_{pst}-*pgs*). To obtain γ-PGA production by γ-PGA synthetase expression with the phosphate-starvation inducible promoter, the start phosphate concentration was reduced to 0.5 g L^{-1} K_2HPO_4. The cultivations were carried out in 1.3 L bioreactors (BioFlo120, Eppendorf). The γ-PGA concentration and cell dry weight were determined. For *B. subtilis* PG3 the CDW was additionally determined with online measurement by the CGQ.

mutant *B. subtilis* PG3, large variations in the growth behavior as well as in the γ-PGA production were observed (Figures 3, 4). While the OTR measurement for reference strain PG2 (Figure 3A) shows a highly reproducible trend with low deviations in the lag time and the maximum values reached, large variations are observed for the by-product deletion mutant PG3 (Figure 3B). For *B. subtilis* PG3, an 8 h difference in the lag phase was observed, preventing a representative sampling between independent cultures. Moreover, the strong variation in the maximal OTR values of up to 36 mmol L^{-1} h^{-1} as observed for the cultivations one and two that are comparable to the values obtained for the reference strain and only 24.6 mmol L^{-1} h^{-1} highlights growth differences in independent cultivations. Figures

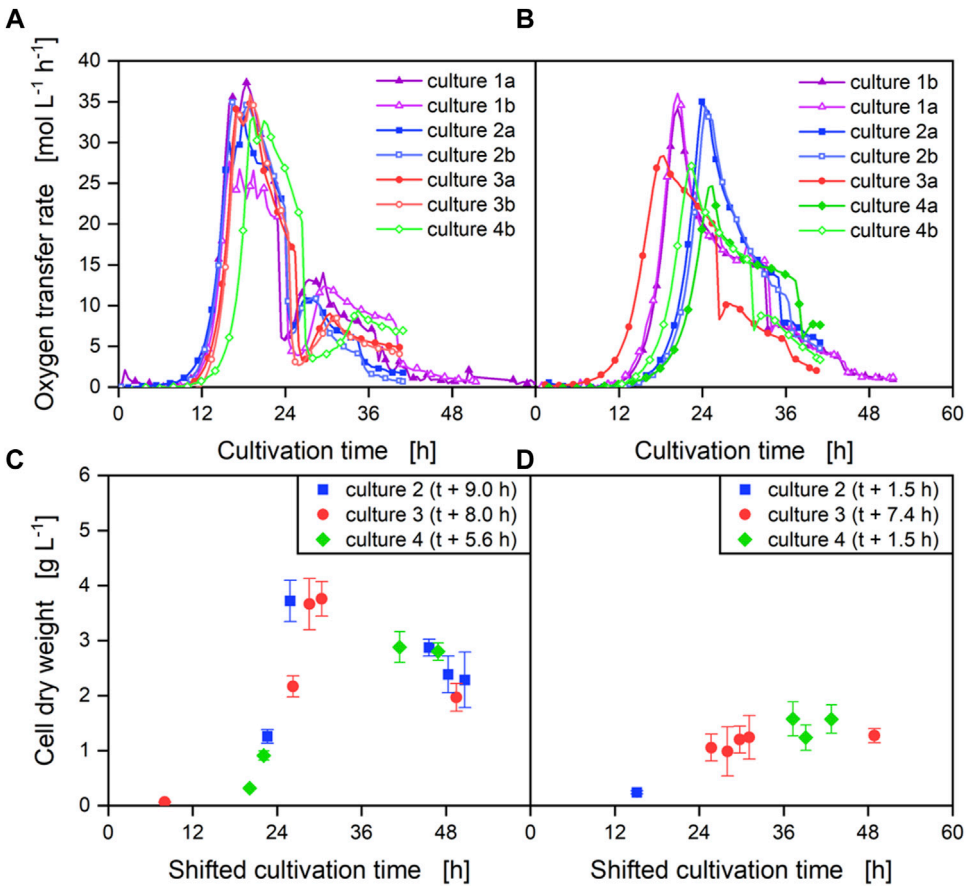

FIGURE 3
Cultivation of *B. subtilis* PG2 and *B. subtilis* PG3 with on-line OTR measurement. In four independent cultivations, the metabolic activity of *B. subtilis* PG2 (parental strain, P_{pst}-*pgs* **(A)** and *B. subtilis* PG3 (by-product pathway deficient strain, P_{pst}-*pgs* **(B)** was followed on-line using oxygen transfer rate measurements. Off-line samples were used to analyze the biomass concentration for both strains [PG2: **(C)**, PG3: **(D)**]. The time axis off the off-line samples was normalized for each experiment to correspond to an OTR exceeding 20 mmol L^{-1} h^{-1} at 24 h elapsed cultivation time (see Supplementary Figure S2).

3C, D show the biomass concentrations of off-line samples for *B. subtilis* PG2 and PG3, respectively that were taken throughout cultivations two to 4. To visualize the growth behaviour, the indicated sampling points in Figures 3C, D are shifted to compensate for the variation in the lag phase. For the reference strain PG2, all data points from independent cultivations fit to each other, resulting in a growth curve that is comparable to the bioreactor cultivation (Figure 2A). For the deletion mutant PG3, a high variation between the cultivations was observed that is in line with the differences in the maximal OTR values for PG3. In cultivation 2, where a high maximal OTR was reached, a high biomass concentration of up to 4 g L^{-1} was measured that was comparable to the biomass obtained for the reference. In contrast, the biomass determination in cultivation 3 and 4, in which lower maximal OTR values were reached, resulted in values of only up to 1.6 g L^{-1}. The growth behavior that was observed for these two cultivations was comparable to the growth behavior observed in the bioreactor cultivation (Figure 2B). Conclusively, the cultivation conditions for a multiple knockout mutant using low phosphate concentrations are very sensitive to any perturbations.

The on-line measurements of the two strains *B. subtilis* PG2 and PG3 are summarized in Figure 4. For the calculation of mean and standard deviation of seven independent OTR measurements and three independent viscosity measurements per strain, the time axis was normalized for each experiment to obtain an OTR exceeding 20 mmolL^{-1} h^{-1} at 24 h elapsed cultivation time. Using these shifted OTR curves, reproducible results with low standard deviation for the respiration activity were obtained. For the reference strain PG2, a sharp drop in the OTR curve was observed after 28.5 h from the maximal OTR of approx. 33 mmol L^{-1} h^{-1} to only 5 mmol L^{-1} h^{-1} after 34.5 h. This drop likely corresponds to the depletion of glucose. From 34.5 h to 38.5 h, the OTR increases again to reach a second peak of 9.5 mmol L^{-1} h^{-1}, most likely indicating the uptake of overflow metabolites such as acetate, 2,3-butanediol, and lactate produced during the first growth phase on glucose. The course of the OTR matches the determination of by-products as the highest concentrations of acetate and lactate were determined after approx. 30 h and glucose was only detected up to 30 h (Supplementary Figure S1). Importantly, the by-product with the highest concentration reaching 3 g L^{-1} was lactate. The lactate synthesis was not yet prevented in the by-product deletion

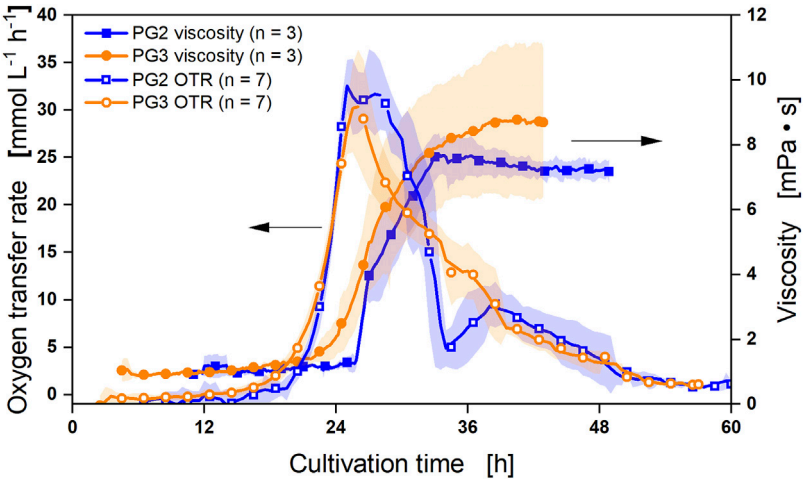

FIGURE 4
Online measurement of the oxygen transfer rate and viscosity during γ-PGA synthesis by *B. subtilis* PG2 and PG3. The respiration activity as indicated by the OTR was investigated for reference strain *B. subtilis* PG2 and deletion mutant *B. subtilis* PG3. The γ-PGA production was determined as measured viscosity. The standard deviation is shown as transparent shadow of seven biological replicates for the OTR and three biological replicates for the viscosity.

mutant. Furthermore, the production of acetoin could not be detected due to insufficient resolution of the employed HPLC method in cultivations with MOPS buffer. From 50 h onwards, none of the investigated metabolites was detectable and the respiratory activity is near to 0 mmol L^{-1} h^{-1} indicating the end of the batch cultivation (Supplementary Figure S1, 2). For the deletion mutant PG3, the initial increase in OTR is comparable to the reference strain. However, the maximal OTR is lower, reaching only 30 mmol L^{-1} h^{-1} and exhibiting a higher standard deviation that is due to the differences in the growth as stated above (Figure 3). Moreover, the slope of the OTR drop following the maximal OTR is lower when compared to PG2, resulting in a broader shoulder of the OTR curve with a smaller second peak between 34.5 h and 38.5 h. These findings correspond to a lower by-product synthesis. Acetate production was observed for PG3 (Supplementary Figure S1) despite deletion of the *pta* gene, whose gene product catalyzes the first step in the annotated acetate synthesis pathway of *B. subtilis*. The acetate kinase might be a beneficial target to avoid acetate formation, although we do not have a suggestion which other enzyme activity besides Pta provides acetyl-P. The production and subsequent consumption of 0.9 g L^{-1} acetate by PG3 matches the OTR signal.

γ-PGA synthesis was monitored by on-line viscosity measurements (Figure 4). For reference PG2, the highest viscosity was obtained after 33 h reaching 7.7 mPa·s. This time point corresponds to the transition from glucose to by-product consumption, as deduced from the OTR. From 33 h on, a rather constant viscosity was observed for strain PG2 decreasing to 7.2 mPa·s at the end of the fermentation. The results indicate that strain *B. subtilis* PG2 does not produce γ-PGA during growth on overflow metabolites. Notably, a low standard deviation was observed for the online viscosity measurements with strain PG2. In contrast, viscosity measurement for the deletion strain PG3 significantly varied between the three measurements ranging from high maximal values of 11 mPa·s to lower maximal values of 7.1 mPa·s that are in the range of the reference strain. Still, the online viscosity measurements for reference PG2 and deletion strain PG3 resulting in a higher viscosity for PG3 correspond to the results obtained with GPC and CTAB measurements (Figure 2). As for the reference, the highest increase of viscosity for PG3 is observed during growth on glucose, resulting in a high slope for the viscosity curve up to 33 h. Due to the elongated growth phase of strain PG3, the viscosity further increases slightly until the end of the measurement, reaching a maximum of 8.8 mPa·s. While higher γ-PGA production by PG3 in minimal medium with phosphate limitation could be confirmed, the low reproducibility hints to the fact that the use of the phosphate-starvation promoter and hence, phosphate limitation should be avoided to stabilize γ-PGA production.

3.2 Intracellular metabolite analysis

The metabolite profiles for the reference strain *B. subtilis* Δspo, the deletion mutant *B. subtilis* ΔBP, the γ-PGA-producing reference *B. subtilis* PG2, and the γ-PGA-producing deletion mutant *B. subtilis* PG3 were compared (Figure 5). The metabolite data of the two deletion strains *B. subtilis* ΔBP and *B. subtilis* PG3 is highly similar, showing that the γ-PGA production has a minor effect on the metabolite concentrations. This observation is likely due to the low γ-PGA titer that is reached for the strains expressing the γ-PGA synthetase under control of the phosphate-starvation inducible promoter P_{pst}. Still, differences in the concentrations of the direct γ-PGA precursors (iso-)citrate, 2-oxoglutarate, and glutamate are observed. These precursor concentrations are slightly decreased for the two γ-PGA producing strains, whereas the concentrations of these metabolites are increased in the deletion mutant *B. subtilis* PG3 compared to *B. subtilis*

10.3389/frfst.2023.1111571

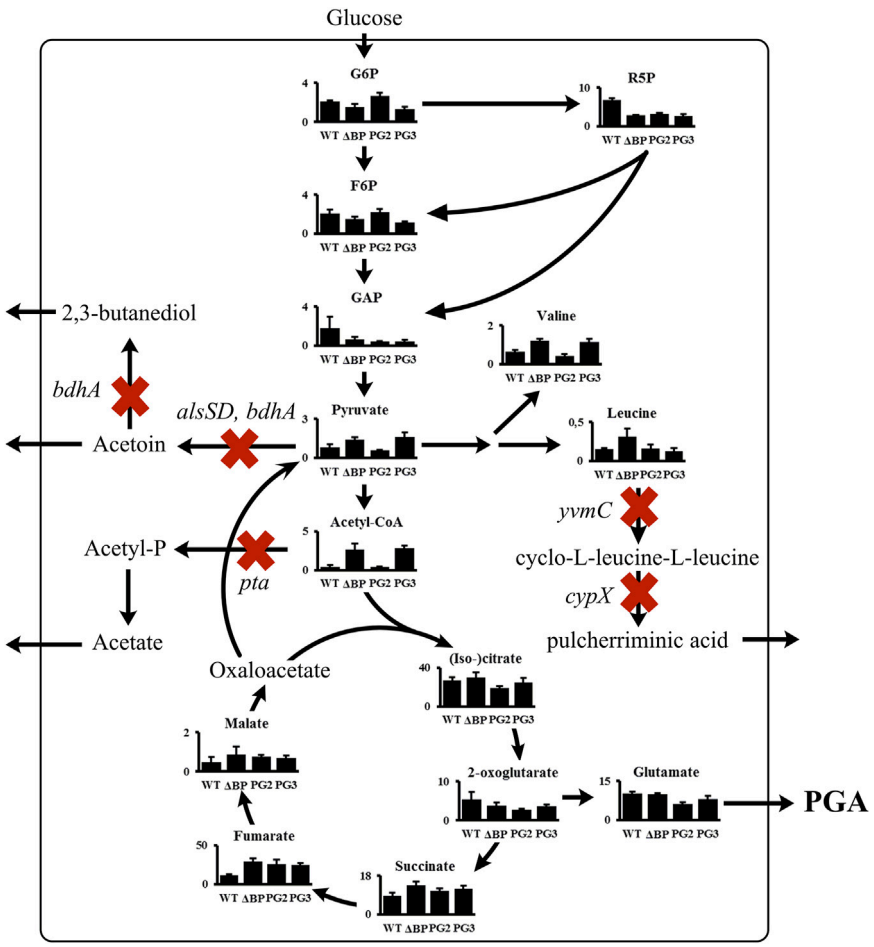

FIGURE 5
Intracellular metabolite analysis for deletion mutants. The non-γ-PGA producing *B. subtilis* Δspo (WT), *B. subtilis* Δ*alsSD* Δ*bdhA* Δ*pta* Δ*yvmC* Δ*cypX* (ΔBP), *B. subtilis* PG2 (P_{pst}-*pgs*), and *B. subtilis* PG3 (ΔBP P_{pst}-*pgs*) were analyzed.

PG2. Hence, the gene deletions resulted in the desired effect of increasing the precursor supply. The measured concentrations of glycolysis intermediates show an accumulation of acetyl-CoA and pyruvate for the deletion mutants. These findings indicate that the activity of the citrate synthase likely is the limiting step for the flux towards glutamate. Since the concentration of the direct γ-PGA precursors citrate, 2-OG and glutamate is nearly as high in the γ-PGA producing deletion strain PG3 as in the γ-PGA-negative strain ΔBP, the expression or activity of the PGA synthetase is most likely the limiting factor in γ-PGA production for the deletion strain PG3. Hence, the investigated gene deletions must be combined with a higher expression level of the PGA synthetase to optimize the γ-PGA production in engineered deletion mutants with glucose as sole carbon source.

3.3 γ-PGA production with *B. subtilis* ΔBP using a constitutive promoter for pgs

To maximize the benefit of the increased precursor supply in the deletion mutants, the weak promoter P_{pst} was replaced by the strong, constitutive synthetic promoter PV35.26 (Halmschlag et al., 2020b). As for the use of the phosphate-starvation promoter, two strains, the reference strain *B. subtilis* PG32 and the by-product deletion strain *B. subtilis* PG33 both expressing the *pgs* genes under control of promoter PV35.26, were investigated for growth and γ-PGA production in glucose batch fermentations (Figure 6). Independent of the promoter used for PGA synthetase expression, a higher γ-PGA titer was reached for the deletion mutant with blocked by-product synthesis pathways. The γ-PGA titer was 3-fold higher for *B. subtilis* PG33 compared to the reference, reaching 0.57 g L^{-1} γ-PGA. Interestingly, a higher growth rate was observed for the deletion mutant being 0.47 h^{-1} compared to a growth rate of 0.3 h^{-1} for *B. subtilis* PG32. In comparison to the phosphate-starvation medium, a significantly higher biomass concentration was obtained with the new strains in minimal medium containing increased concentrations of phosphate. The higher biomass concentration and γ-PGA titer highlight the benefit of a stronger, constitutive promoter for γ-PGA production in minimal medium with glucose as sole carbon source.

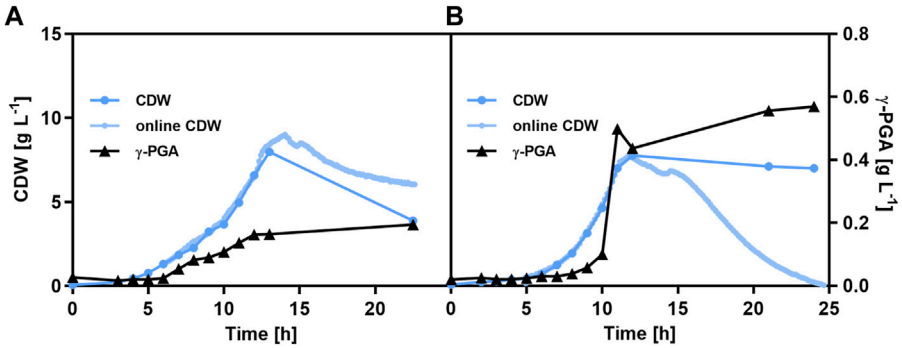

FIGURE 6
γ-PGA production in glucose minimal medium using strains carrying the PGA synthetase under the control of a constitutive promoter. Batch cultivation of *B. subtilis* PG32 (parental strain, $P_{PV35.26}$-*pgs*; **(A)** and *B. subtilis* PG33 (by-product pathway deficient strain, $P_{PV35.26}$-*pgs*; **(B)**. The cultivations were carried out in 1.3 L bioreactors (BioFlo120, Eppendorf). The γ-PGA concentration as determined by the CTAB assay and cell dry weight were determined. The biomass concentration was determined offline by OD_{600} measurements and online by light scattering (CGQ).

3.4 Deletion of lactate dehydrogenase and production medium E

Even with the constitutive promoter PV35.26 (Halmschlag et al., 2020b), the γ-PGA production obtained with the deletion strain *B. subtilis* PG33 is below 1 g L^{-1}. A variant of the xylose-inducible promoter P_{xyl} resulted in the highest γ-PGA concentrations with either glucose or xylose as carbon source. Further, online viscosity measurement with the promoter P_{xyl} resulted in a high viscosity of up to 40 mPa·s in a minimal medium with xylose as sole carbon source, highlighting the high potential of the xylose inducible promoter (Halmschlag et al., 2020a). Importantly, the promoter is inducible by xylose but in contrast to the native P_{xyl} promoter for the *xylAB* operon, it is not repressed by glucose as the CcpA binding site responsible for the repression is missing. In addition to previous gene deletions in strain ΔBP, the lactate dehydrogenase gene *ldh* was deleted to prevent the production of lactate that was observed as a major by-product for the constructed strains. Moreover, the *xylAB* operon responsible for xylose metabolization was deleted in both the Δspo and ΔBP background to prevent depletion of the promoter inducing agent during cultivation, ultimately leading to the construction of *B. subtilis* PG4 and PG5. The xylose inducible promoter was integrated into *B. subtilis* PG4 and PG5, yielding the γ-PGA-producing strains *B. subtilis* PG44 and *B. subtilis* PG55. To identify the maximal γ-PGA production capacities of the engineered strains, the glucose minimal medium was replaced by the known γ-PGA production medium, Medium E, which was reported to enable γ-PGA production of up to 53 g L^{-1} in *B. licheniformis* ATCC9945 (Mitsunaga et al., 2016). However, only 30 g L^{-1} glycerol were used for this experiment as compared to 80 g L^{-1} reported by Mitsunaga et al. (2016), aiming to reach a higher product yield as reported in the literature. With these modifications of the *pgs* expression system and the cultivation medium, we aimed to harness the theoretical potential of increased γ-PGA synthesis in the by-product deficient strain albeit the so far mediocre production titers.

Only a slight difference in biomass formation of *B. subtilis* PG44 and PG55 was observed during cultivation in modified Medium E, with *B. subtilis* PG44 reaching a higher final optical density as compared to PG55 (Figure 7A). Whereas the pH of the medium inoculated with *B. subtilis* PG44 started to increase mildly after the first 24 h of cultivation, a steep drop in pH was observed in case of *B. subtilis* PG55 at that time point. Within 24 h, the pH of the medium cultivated with *B. subtilis* PG55 decreased from 6.8 to 5.3 despite initial buffering with 41.9 g L^{-1} MOPS (Figure 7A). Glycerol was used instead of glucose as main carbon source in modified Medium E. According to Mitsunaga et al. (2016), γ-PGA synthesis is increased in *B. licheniformis* ATCC9945 cultivated in Medium E with glycerol, compared to cultivation with glucose. *B. subtilis* PG44 consumed the available 30 g L^{-1} of glycerol within 48 h of cultivation, whereas in medium cultivated with *B. subtilis* PG55, 1.7 g L^{-1} glycerol was detected even after 72 h. After 48 h of cultivation which resembles the point of carbon source depletion of *B. subtilis* PG44, a γ-PGA titer of 9.9 g L^{-1} with a molecular weight of 2,125 kDa was reached in this strain background. However, a γ-PGA titer of 13.2 g L^{-1} with a molecular weight of 3,027 kDa was detected for deletion strain *B. subtilis* PG55 after 48 h, which further increased to 14.5 g L^{-1} after 72 h of cultivation (Figure 7C). Notably, the molecular weight of γ-PGA produced by *B. subtilis* PG44 reached its maximum of 4,905 kDa after 24 h of cultivation and gradually decreased over the course of the next 48 h. In contrast, the molecular weight of γ-PGA provided by *B. subtilis* PG55 was largely unaffected during cultivation (Figure 7C). Since *B. subtilis* PG55 produced a higher γ-PGA titer as compared to *B. subtilis* PG44 even without glycerol depletion, circumventing the pH decrease and potential metabolic burden exerted by the acidic environment may further improve γ-PGA production. Ma et al. (2018) have reported a similar decrease in culture pH of a *B. subtilis* strain with reduced overflow metabolism. The authors have concluded that with the prevention of acetoin production, pyruvate accumulates intracellularly and therefore accelerates acetate formation. Since in *B. subtilis* PG55 the synthesis of acetyl-phosphate and therefore the acetate precursor formation is blocked through the deletion of *pta*, excess pyruvate may not be redistributed and therefore might accumulate to toxic levels. Indeed, extracellular pyruvate levels were significantly higher in cell free culture supernatant of *B. subtilis* PG55 as compared to *B. subtilis* PG44. After 72 h of cultivation, an

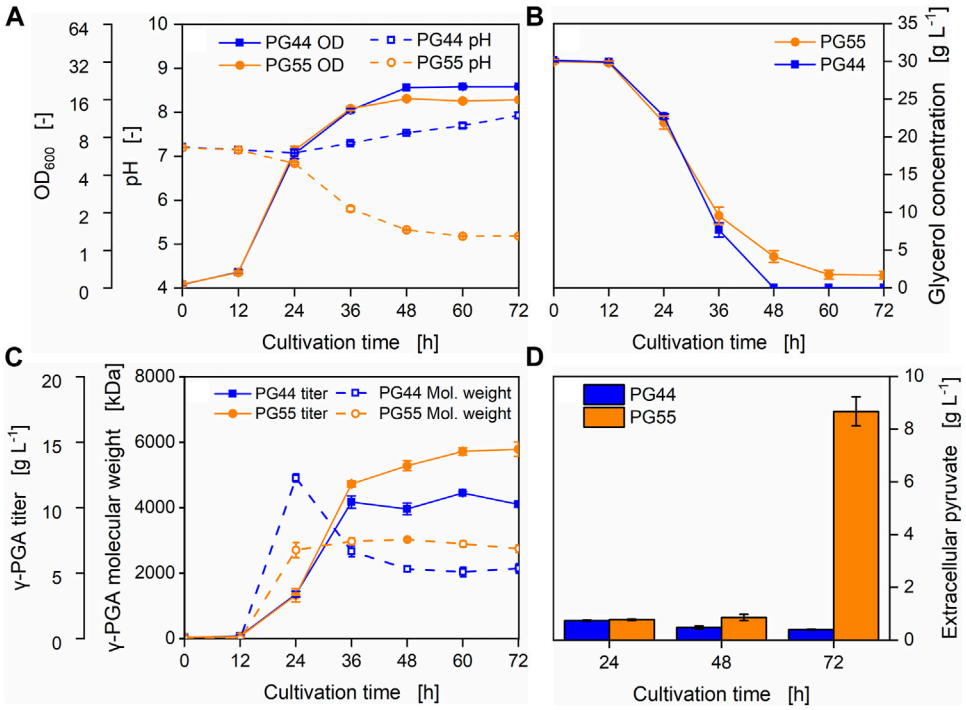

FIGURE 7
γ-PGA production in Medium E using strains carrying the PGA synthetase under the control of a xylose inducible promoter. Batch cultivation of *B. subtilis* PG44 (parental strain, P_{xyl}-*pgs*) and PG55 (by-product pathway deficient strain, P_{xyl}-*pgs*). The cultivations were carried out in 500 mL shake flasks. To induce γ-PGA synthesis, 30 g L^{-1} xylose was added at the beginning of the experiment. During cultivation, the OD_{600} and pH **(A)**, glycerol concentration **(B)**, γ-PGA titer and the molecular weight **(C)** were monitored. Moreover, the concentration of extracellular pyruvate was quantified **(D)**.

extracellular pyruvate concentration of 8.7 g L^{-1} pyruvate was reached in the by-product deficient strain as compared to 0.4 g L^{-1} in culture supernatants of the parental strain, resembling a 22-times increase in concentration. This high pyruvate concentration in combination with 14.4 g L^{-1} of produced γ-PGA can be explained by the fact that glycerol is accompanied by citrate and glutamate as available carbon sources in modified Medium E. Notably, the pH of cultures of *B. subtilis* PG55 already decreased after 48 h of cultivation, alongside an extracellular pyruvate concentration of 0.85 g L^{-1} as compared to 0.4 g L^{-1} in cultures of the parental strain *B. subtilis* PG44. The steep increase of extracellular pyruvate within the next 12 h associated with the deletion mutant may be explained by cell lysis and subsequent release of the intracellularly accumulating metabolite.

The presented results demonstrate the high potential of engineered *B. subtilis* with reduced by-product synthesis for improved γ-PGA production with either glucose or glycerol as sole carbon source in minimal medium.

4 Discussion

The cost-efficient γ-PGA production without addition of γ-PGA precursors such as glutamate or citrate requires the rerouting of the metabolic flux towards glutamate. The *de novo* glutamate synthesis was reported as bottleneck for γ-PGA production without addition of exogenous glutamate as several studies reported significantly increased γ-PGA titers by addition of exogenous glutamate (Lin et al., 2016; Mitsunaga et al., 2016). Yao et al. investigated the origin of carbon in γ-PGA using 13C-labeled glucose and L-glutamate as carbon sources for a *B. subtilis* producer, showing that only up to 9% of the γ-PGA was derived from glucose (Yao et al., 2010). Here, we engineered γ-PGA producing *B. subtilis* 168 derivative strains with or without deletions of by-product synthesis pathways to efficiently direct the carbon flux from glucose towards γ-PGA. The presented results demonstrate the high potential of metabolic flux rerouting with a 3.7-fold or 1.5-fold increase in γ-PGA production for the deletion mutant in glucose minimal medium or modified Medium E, respectively. Integration of the engineered strains into optimized PGA production processes has the potential to decrease the substrate cost for PGA synthesis. Feng et al. (2015) previously reported improved γ-PGA synthesis with an engineered *B. amyloliquefaciens* strain that lacked the genes *eps*, *sac*, *lps*, and *pta*. The γ-PGA production with the reported strain slightly increased from 3.8 to 4.15 g L^{-1}. The authors observed a larger increase to 9.18 g L^{-1} by additional deletion of genes encoding γ-PGA degrading enzymes. Further, the beneficial effects on the deletion of genes *odhAB* or *sucCD*, encoding the 2-oxoglutarate dehydrogenase and the succinyl-CoA synthetase, respectively, was reported (Massaiu et al., 2019). The deletions successfully channeled the metabolic flux towards glutamate and increased the γ-PGA titer with citrate and glucose as carbon sources. The metabolome analysis carried out here identified the citrate synthase as major bottleneck

for cultivations with glucose as sole carbon source. The variations of the influence of investigated engineering strategies throughout various studies underline that the impact of gene deletion strongly depends on the investigated strain and culture conditions.

The improved γ-PGA synthesis with the by-product deletion mutant was not only demonstrated with glucose as carbon source but also in modified Medium E. In this modified version of the medium, only 30 g L^{-1} glycerol was used as compared to commonly used 80 g L^{-1}, aiming for an increased γ-PGA yield due to the streamlined carbon metabolism and anticipated enhanced *de novo* glutamate synthesis. Using the xylose-inducible promoter P_{xyl}, the γ-PGA titer produced in modified Medium E by the by-product deficient strain *B. subtilis* PG55 was increased by 41% (14.46 g L^{-1} vs. 10.24 g L^{-1} after 72 h) as compared to the parental strain *B. subtilis* PG44. Moreover, the product yield was improved from 0.33 $g_{\gamma\text{-PGA}}/g_{glycerol}$ to 0.51 $g_{\gamma\text{-PGA}}/g_{glycerol}$ provided by the newly generated knockout strain *B. subtilis* PG55 in this medium highlighting the improved synthesis capability of the deletion mutant even with reduced substrate concentration. Limited metabolization of available glycerol might indicate a metabolic arrest of *B. subtilis* PG55 induced by the prominent decrease in culture pH, which is also depicted by the reduced maximal optical density of the strain. Accumulation of extracellular pyruvate poses one possible explanation for this observation. Although the acidification of the medium may be addressed by active pH control using a bioreactor setup, this has no effect on the metabolic imbalance present in the deletion mutant. Future research approaches will focus on stabilizing the culture pH by rerouting carbon flux around bottlenecks identified in this work, thereby avoiding accumulation of potential acidic metabolites. Notably, the γ-PGA titers obtained in this study ranging from less than 1 g L^{-1} in glucose minimal medium to 14.46 g L^{-1} in modified medium E are lower than reported titers of more than 40 g L^{-1} (Zhao et al., 2013; Zhang et al., 2019), indicating the potential for further optimization of production strain and cultivation conditions. Despite the lower production, the genetic streamlining of the carbon metabolism through deletion of by-product formation pathways improved both γ-PGA yield and titer in the deletion mutant independent of the promotor of synthetase genes and the used medium for polymer synthesis. Furthermore, the metabolic bottlenecks identified in this work will guide the future strain optimization that will be combined with optimized cultivation conditions.

The detailed metabolome analysis as well as the detection of accumulating pyruvate for deletion mutants in Medium E identify the citrate synthase as important metabolic engineering target to further optimize the γ-PGA production with by-product deletion mutants. The conversion of this overflow metabolite into a TCA cycle intermediate can further channel the metabolic flux towards γ-PGA precursor molecules. Strengthening the flux of pyruvate into the TCA cycle and therefore towards γ-PGA production will be object of future studies. The advances in γ-PGA product titer and yield for the deletion mutants even in an acidic environment highlight the potential of the engineered strains to harness the already increased precursor supply induced by a reduction of overflow metabolism. Interestingly, by-product formation was not completely abolished by deletion of the respective pathways. Lactate, acetoin and acetate continued to be produced by *B. subtilis* PG55 in modified Medium E due to unknown metabolic pathways. This observation is in unison with the work of Zhu et al., who detected acetate formation in *Corynebacterium glutamicum* even in the absence of the related metabolic synthesis pathways (Zhu et al., 2013). In *Escherichia coli*, the two-electron flavoprotein pyruvate oxidase PoxB catalyses the decarboxylation of pyruvate to acetate and CO_2 independent of the classic synthesis route involving Pta and Ack (Li et al., 2007). In case of *Streptococcus pneumoniae*, the analogous pyruvate oxidase SpxB catalyses the synthesis of acetyl-phosphate from pyruvate, which is then further converted to acetate (Echlin et al., 2016). Based on these examples it can be hypothesized that a similar system is present in engineered *B. subtilis* 168, although so far only marginally investigated. According to the NCBI gene database, an acetyl-phosphate generating pyruvate oxidase is indeed present in *B. subtilis* 168 at location NC_000963.3 (BP 488830 to 490,554, gene ID 938239). The genomic location is annotated as putative pyruvate oxidase YdaP in *B. subtilis* 168 in the SubtiWiki database (Pedreira et al., 2022). YdaP has been identified as an acetate forming pyruvate oxidase in *Bacillus licheniformis* 9A, highlighting its potential role in acetate or acetyl-phosphate synthesis in the constructed deletion mutant *B. subtilis* PG55 (Wani Lako et al., 2018). Since *B. subtilis* PG55 is only deficient in *pta* which is responsible for the conversion of acetyl-CoA to acetyl-phosphate, acetate formation through AckA might occur based on a Pta-independent source of acetyl-phosphate as provided by a *B. subtilis* pyruvate oxidase. The deletion of putative pyruvate oxidase genes or the acetate kinase gene *ackA* with their respective effect on acetate production in *B. subtilis* PG55 will be object of future research.

The presence of acetoin produced by *B. subtilis* deficient in *alsSD* might indicate a novel synthesis route. Previously, a successful prevention of acetoin formation upon deletion of the *alsSD* operon was reported (Ma et al., 2018). The overflow metabolism of *B. subtilis* not only offers the possibility to redirect accumulating pyruvate into neutral fermentation products but also enables regeneration of NAD + through the synthesis of lactate and 2,3-butanediol (Nakano et al., 1997). Deletion of these synthesis routes might therefore result in an imbalance in redox metabolism, hindering cell growth and ultimately γ-PGA production. Indeed, redox state alteration in *B. subtilis* has already been shown to accelerate the production of NAD + -dependent products such as acetoin (Zhang et al., 2014). However, introduction of an NADH oxidase into by-product deficient *B. subtilis* showed no effect in synthesis of *N*-acetylglucosamine (Gu et al., 2019). Investigations whether the introduction of an NADH oxidase into the engineered *B. subtilis* mutants reported in this study influences growth or γ-PGA production will be subject of our future work.

Aiming at a cost-efficient and sustainable γ-PGA production, the presented metabolic engineering results demonstrate the high potential of *B. subtilis* as production host. The provided information

will be used to guide metabolic engineering strategies in further studies to optimize γ-PGA production with either glucose as sole carbon source or in the γ-PGA production Medium E.

Data availability statement

The original contributions presented in the study are included in the article/Supplementary Material, further inquiries can be directed to the corresponding authors.

Author contributions

BH, FV, and LB conceived and designed the study. BH, FV, and RH performed the experiments and drafted the manuscript. RH and JB contributed to the design and data analysis of on-line measurements. SP and EF contributed to the design and data analysis of metabolomics experiments. All authors read and approved the final manuscript.

Funding

This work was funded by the Deutsche Forschungsgemeinschaft (DFG) within the International Research Training Group 1628, "Selectivity in Chemo and Biocatalysis (SeleCa)" and by the PhD Scholarship program of The German Federal Environmental Foundation (Deutsche Bundesstiftung Umwelt DBU).

Conflict of interest

The authors declare that the research was conducted in the absence of any commercial or financial relationships that could be construed as a potential conflict of interest.

Publisher's note

All claims expressed in this article are solely those of the authors and do not necessarily represent those of their affiliated organizations, or those of the publisher, the editors and the reviewers. Any product that may be evaluated in this article, or claim that may be made by its manufacturer, is not guaranteed or endorsed by the publisher.

Supplementary material

The Supplementary Material for this article can be found online at: https://www.frontiersin.org/articles/10.3389/frfst.2023.1111571/full#supplementary-material

References

Amer, B., and Baidoo, E. E. K. (2021). Omics-driven biotechnology for industrial applications. *Front. Bioeng. Biotechnol.* 9, 613307. doi:10.3389/fbioe.2021.613307

Anderlei, T., and Büchs, J. (2001). Device for sterile online measurement of the oxygen transfer rate in shaking flasks. *Biochem. Eng. J.* 7 (2), 157–162. doi:10.1016/s1369-703x(00)00116-9

Anderlei, T., Zang, W., Papaspyrou, M., and Büchs, J. (2004). Online respiration activity measurement (OTR, CTR, RQ) in shake flasks. *Biochem. Eng. J.* 17 (3), 187–194. doi:10.1016/s1369-703x(03)00181-5

Bovy, A., Schijlen, E., and Hall, R. D. (2007). Metabolic engineering of flavonoids in tomato (Solanum lycopersicum): The potential for metabolomics. *Metabolomics* 3, 399–412. doi:10.1007/s11306-007-0074-2

Echlin, H., Frank, M. W., Iverson, A., Chang, T. C., Johnson, M. D., Rock, C. O., et al. (2016). Pyruvate oxidase as a critical link between metabolism and capsule biosynthesis in Streptococcus pneumoniae. *Streptococcus Pneumoniae. PLoS Pathog.* 12 (10), e1005951. doi:10.1371/journal.ppat.1005951

Feng, J., Gu, Y., Quan, Y., Cao, M., Gao, W., Zhang, W., et al. (2015). Improved poly-γ-glutamic acid production in *Bacillus amyloliquefaciens* by modular pathway engineering. *Metab. Eng.* 32, 106–115. doi:10.1016/j.ymben.2015.09.011

Feng, J., Gu, Y., Sun, Y., Han, L., Yang, C., Zhang, W., et al. (2014). Metabolic engineering of *Bacillus amyloliquefaciens* for poly-gamma-glutamic acid (γ-PGA) overproduction. *Microb. Biotechnol.* 7 (5), 446–455. doi:10.1111/1751-7915.12136

Feng, J., Quan, Y., Gu, Y., Liu, F., Huang, X., Shen, H., et al. (2017). Enhancing poly-gamma-glutamic acid production in Bacillus amyloliquefaciens by introducing the glutamate synthesis features from Corynebacterium glutamicum. *Microb. Cell Fact.* 16 (1), 88. doi:10.1186/s12934-017-0704-y

Gold, N. D., Gowen, C. M., Lussier, F. X., Cautha, S. C., Mahadevan, R., and Martin, V. J. (2015). Metabolic engineering of a tyrosine-overproducing yeast platform using targeted metabolomics. *Microb. Cell Fact.* 14, 73. doi:10.1186/s12934-015-0252-2

Gu, Y., Lv, X., Liu, Y., Li, J., Du, G., Chen, J., et al. (2019). Synthetic redesign of central carbon and redox metabolism for high yield production of N-acetylglucosamine in Bacillus subtilis. *Metab. Eng.* 51, 59–69. doi:10.1016/j.ymben.2018.10.002

Halmschlag, B., Hoffmann, K., Hanke, R., Putri, S. P., Fukusaki, E., Büchs, J., et al. (2020a). Comparison of isomerase and weimberg pathway for γ-PGA production from xylose by engineered Bacillus subtilis. *Bacillus Subtilis. Front. Bioeng. Biotechnol.* 7, 476. doi:10.3389/fbioe.2019.00476

Halmschlag, B., Putri, S. P., Fukusaki, E., and Blank, L. M. (2020b). Identification of key metabolites in poly-gamma-glutamic acid production by tuning gamma-PGA synthetase expression. *Front. Bioeng. Biotechnol.* 8, 38. doi:10.3389/fbioe.2020.00038

Halmschlag, B., Steurer, X., Putri, S. P., Fukusaki, E., and Blank, L. M. (2019). Tailor-made poly-gamma-glutamic acid production. *Metab. Eng.* 55, 239–248. doi:10.1016/j.ymben.2019.07.009

Harwood, C. R., and Cutting, S. M. (1990). *Molecular biological methods for* Bacillus. Wiley.

Hoffmann, K., Halmschlag, B., Briel, S., Sieben, M., Putri, S., Fukusaki, E., et al. (2022). Online measurement of the viscosity in shake flasks enables monitoring of gamma-PGA production in depolymerase knockout mutants of Bacillus subtilis with the phosphate-starvation inducible promoter Ppst. *Biotechnol. Prog.* 39, e3293. doi:10.1002/btpr.3293

Kato, Y., Inabe, K., Hidese, R., Kondo, A., and Hasunuma, T. (2022). Metabolomics-based engineering for biofuel and bio-based chemical production in microalgae and cyanobacteria: A review. *Bioresour. Technol.* 344, 126196. doi:10.1016/j.biortech.2021.126196

Leonard, C. G., Housewright, R. D., and Thorne, C. B. (1958). Effects of some metallic ions on glutamyl polypeptide synthesis by Bacillus subtilis. *Bacillus Subtilis. J. Bacteriol.* 76, 499–503. doi:10.1128/JB.76.5.499-503.1958

Li, M., Yao, S., and Shimizu, K. (2007). Effect of poxB gene knockout on metabolism in *Escherichia coli* based on growth characteristics and enzyme activities. *World J. Microbiol. Biotechnol.* 23 (4), 573–580. doi:10.1007/s11274-006-9267-5

Li, M., Zhu, X., Yang, H., Xie, X., Zhu, Y., Xu, G., et al. (2020). Treatment of potato starch wastewater by dual natural flocculants of chitosan and poly-glutamic acid. *J. Clean. Prod.* 264, 121641. doi:10.1016/j.jclepro.2020.121641

Li, X., Yang, H., Zhou, M., Zhan, Y., Liu, J., Yan, D., et al. (2021). A novel strategy of feeding nitrate for cost-effective production of poly-γ-glutamic acid from crude glycerol by Bacillus licheniformis WX-02. *Biochem. Eng. J.* 176, 108156. doi:10.1016/j.bej.2021.108156

Lin, B., Li, Z., Zhang, H., Wu, J., and Luo, M. (2016). Cloning and expression of the gamma-polyglutamic acid synthetase gene *pgsBCA* in *Bacillus subtilis* WB600. *Biomed. Res. Int.* 2016, 3073949. doi:10.1155/2016/3073949

Lin, B., and Tao, Y. (2017). Whole-cell biocatalysts by design. *Microb. Cell Fact.* 16 (1), 106. doi:10.1186/s12934-017-0724-7

Ma, W., Liu, Y., Shin, H.-d., Li, J., Chen, J., Du, G., et al. (2018). Metabolic engineering of carbon overflow metabolism of *Bacillus subtilis* for improved N-acetyl-glucosamine production. *Bioresour. Technol.* 250, 642–649. doi:10.1016/j.biortech.2017.10.007

Massaiu, I., Pasotti, L., Sonnenschein, N., Rama, E., Cavaletti, M., Magni, P., et al. (2019). Integration of enzymatic data in *Bacillus subtilis* genome-scale metabolic model improves phenotype predictions and enables *in silico* design of poly-gamma-glutamic acid production strains. *Microb. Cell Fact.* 18 (1), 3. doi:10.1186/s12934-018-1052-2

Meselson, M., and Yuan, R. (1968). DNA restriction enzyme from *E. coli*. *Nature* 217 (5134), 1110–1114. doi:10.1038/2171110a0

Messing, J., Crea, R., and Seeburg, P. H. (1981). A system for shotgun DNA sequencing. *Nucleic Acids Res.* 9 (2), 309–321. doi:10.1093/nar/9.2.309

Mitsunaga, H., Meissner, L., Palmen, T., Bamba, T., Büchs, J., and Fukusaki, E. (2016). Metabolome analysis reveals the effect of carbon catabolite control on the poly(γ-glutamic acid) biosynthesis of *Bacillus licheniformis* ATCC 9945. *J. Biosci. Bioeng.* 121 (4), 413–419. doi:10.1016/j.jbiosc.2015.08.012

Nakano, M. M., Dailly, Y. P., Zuber, P., and Clark, D. P. (1997). Characterization of anaerobic fermentative growth of *Bacillus subtilis*: Identification of fermentation end products and genes required for growth. *J. Bacteriol.* 179 (21), 6749–6755. doi:10.1128/jb.179.21.6749-6755.1997

Park, S.-B., Sung, M.-H., Uyama, H., and Han, D. K. (2021). Poly(glutamic acid): Production, composites, and medical applications of the next-generation biopolymer. *Prog. Polym. Sci.* 113, 101341. doi:10.1016/j.progpolymsci.2020.101341

Pedreira, T., Elfmann, C., and Stulke, J. (2022). The current state of SubtiWiki, the database for the model organism Bacillus subtilis. *Bacillus Subtilis. Nucleic Acids Res.* 50 (D1), D875–D882. doi:10.1093/nar/gkab943

Pereira, A. E. S., Sandoval-Herrera, I. E., Zavala-Betancourt, S. A., Oliveira, H. C., Ledezma-Pérez, A. S., Romero, J., et al. (2017). γ-Polyglutamic acid/chitosan nanoparticles for the plant growth regulator gibberellic acid: Characterization and evaluation of biological activity. *Carbohydr. Polym.* 157, 1862–1873. doi:10.1016/j.carbpol.2016.11.073

Putri, S. P., Nakayama, Y., Matsuda, F., Uchikata, T., Kobayashi, S., Matsubara, A., et al. (2013). Current metabolomics: Practical applications. *J. Biosci. Bioeng.* 115 (6), 579–589. doi:10.1016/j.jbiosc.2012.12.007

Scoffone, V., Dondi, D., Biino, G., Borghese, G., Pasini, D., Galizzi, A., et al. (2013). Knockout of pgdS and ggt genes improves γ-PGA yield in B. subtilis. *Biotechnol. Bioeng.* 110 (7), 2006–2012. doi:10.1002/bit.24846

Sieben, M., Hanke, R., and Buchs, J. (2019). Contact-free determination of viscosity in multiple parallel samples. *Sci. Rep.* 9 (1), 8335. doi:10.1038/s41598-019-44859-z

Sirisansaneeyakul, S., Cao, M., Kongklom, N., Chuensangjun, C., Shi, Z., and Chisti, Y. (2017). Microbial production of poly-gamma-glutamic acid. *World J. Microbiol. Biotechnol.* 33 (9), 173. doi:10.1007/s11274-017-2338-y

Uffen Robert, L., and Canale-Parola, E. (1972). Synthesis of pulcherriminic acid by Bacillus subtilis. *J. Bacteriol.* 111 (1), 86–93. doi:10.1128/JB.111.1.86-93.1972

Wani Lako, J. D., Yengkopiong, J. P., Stafford, W. H. L., Tuffin, M., and Cowan, D. A. (2018). Cloning, expression and characterization of thermostable YdaP from *Bacillus licheniformis* 9A. *Acta Biochim. Pol.* 65 (1), 59–66. doi:10.18388/abp.2017_1499

Wenzel, M., and Altenbuchner, J. (2015). Development of a markerless gene deletion system for *Bacillus subtilis* based on the mannose phosphoenolpyruvate-dependent phosphotransferase system. *Microbiology* 161 (10), 1942–1949. doi:10.1099/mic.0.000150

Wenzel, M., Muller, A., Siemann-Herzberg, M., and Altenbuchner, J. (2011). Self-inducible *Bacillus subtilis* expression system for reliable and inexpensive protein production by high-cell-density fermentation. *Appl. Environ. Microbiol.* 77 (18), 6419–6425. doi:10.1128/AEM.05219-11

Yao, J., Xu, H., Shi, N., Cao, X., Feng, X., Li, S., et al. (2010). Analysis of carbon metabolism and improvement of gamma-polyglutamic acid production from *Bacillus subtilis* NX-2. *Appl. Biochem. Biotechnol.* 160 (8), 2332–2341. doi:10.1007/s12010-009-8798-2

Yu, H., Liu, H., Wang, L., Zhang, Y., Tian, H., and Ma, X. (2018). Effect of poly-gamma-glutamic acid on the stability of set yoghurts. *J. Food Sci. Technol.* 55 (11), 4634–4641. doi:10.1007/s13197-018-3404-7

Zhang, C., Wu, D., and Ren, H. (2019). Economical production of agricultural γ-polyglutamic acid using industrial wastes by Bacillus subtilis. *Biochem. Eng. J.* 146, 117–123. doi:10.1016/j.bej.2019.03.013

Zhang, X., Zhang, R., Bao, T., Rao, Z., Yang, T., Xu, M., et al. (2014). The rebalanced pathway significantly enhances acetoin production by disruption of acetoin reductase gene and moderate-expression of a new water-forming NADH oxidase in Bacillus subtilis. *Metab. Eng.* 23, 34–41. doi:10.1016/j.ymben.2014.02.002

Zhao, C., Zhang, Y., Wei, X., Hu, Z., Zhu, F., Xu, L., et al. (2013). Production of ultra-high molecular weight poly-gamma-glutamic acid with Bacillus licheniformis P-104 and characterization of its flocculation properties. *Appl. Biochem. Biotechnol.* 170 (3), 562–572. doi:10.1007/s12010-013-0214-2

Zhu, F., Cai, J., Wu, X., Huang, J., Huang, L., Zhu, J., et al. (2013). The main byproducts and metabolic flux profiling of gamma-PGA-producing strain *B. subtilis* ZJU-7 under different pH values. *J. Biotechnol.* 164 (1), 67–74. doi:10.1016/j.jbiotec.2012.12.009